Materials Horizons

ROYAL SOCIETY OF CHEMISTRY

COMMUNICATION

View Article Online
View Journal | View Issue

Cite this: *Mater. Horiz.*, 2025, **12**, 1274

Received 12th July 2024,
Accepted 14th November 2024

DOI: 10.1039/d4mh00899e

rsc.li/materials-horizons

Functionalization of monolithic MOF thin films with hydrocarbon chains to achieve superhydrophobic surfaces with tunable water adhesion strength†

Evgenia Bogdanova,‡[a] Modan Liu,‡[a] Patrick Hodapp,[b] Angana Borbora,[e] Wolfgang Wenzel,[f] Stefan Bräse,[cd] André Jung,[c] Zheqin Dong,[c] Pavel A. Levkin,[cd] Uttam Manna,*[eg] Tawheed Hashem*[a] and Christof Wöll*[a]

While the accessible pores render an enormous variety of functionalities to the bulk of metal–organic frameworks (MOFs), the outer surfaces exposed by these crystalline materials also offer unique characteristics not available when using conventional substrates. By grafting hydrocarbon chains to well-defined MOF thin films (SURMOFs) prepared using layer-by-layer methods, we were able to fabricate superhydrophobic substrates with static water contact angles over 160°. A detailed theoretical modelling of the hydrocarbon chains grafted on the outer SURMOF surface with well-defined spacing between anchoring points reveals that the grafted hydrocarbon chains behave similarly to polymer brushes during wetting, where conformational entropy is traded with mixing entropy. The chains are coiled and can access many different conformations, as evidenced directly by infrared spectroscopy. The entropic contributions from the coiled state lead to a pronounced reduction of the surface free energy, rendering superhydrophobic properties to the functionalized SURMOFs. On the other side, the water adhesion strength could be decreased by increasing the surface roughness on the nanometer scale.

New concepts

Our paper introduces an innovative and unique approach for creating superhydrophobic surfaces using MOF thin films. This technique employs porous coatings, a fresh idea for achieving hydrophobicity. Although the wetting properties of MOF powder particles have been explored, applying monolithic MOF thin films for this purpose is a groundbreaking concept. Our method produces superhydrophobic surfaces with contact angles significantly higher than those of other coatings with similar roughness. Moreover, we can adjust the water adhesion strength across a wide range.

Introduction

Metal–organic frameworks (MOFs) are crystalline, porous networks composed of inorganic metal nodes and organic linkers.[1] These reticular materials have garnered considerable attention due to their intriguing bulk properties in various fields, including gas capture,[2,3] separation,[4] catalysis,[5,6] and optoelectronics.[7–9] While many of the desirable properties of MOFs result from the interior walls of pores (*e.g.*, attractive interaction with CH_4 or CO_2) or from metal or metal oxo nodes (*e.g.*, H_2 binding), the external surfaces exposed by MOFs have received less attention,[10] mainly due to the small size of powder particles typically obtained from the conventional solvothermal synthesis, which has hindered the characterization of macroscopic MOF surface properties and applications. Recently, the availability of methods for growing high-quality MOF thin films has opened up new possibilities in characterization, *e.g.* the application of indentation methods to determine mechanical characteristics,[11] as well as enabling their integration into (opto)electronic devices.[12] A particularly interesting feature of the outer surfaces of MOFs is the fact that they

[a] *Karlsruhe Institute of Technology (KIT), Institute of Functional Interfaces (IFG), Hermann-von-Helmholtz Platz-1, Eggenstein-Leopoldshafen 76344, Germany. E-mail: christof.woell@kit.edu*
[b] *Karlsruhe Institute of Technology (KIT), Institute for Biological Interfaces – Soft Matter Synthesis Laboratory (IBG3 – SML), Kaiserstrasse 12, Karlsruhe 76131, Germany*
[c] *Karlsruhe Institute of Technology (KIT), Institute of Biological and Chemical Systems (IBCS-FMS), Kaiserstrasse 12, Karlsruhe 76131, Germany*
[d] *Karlsruhe Institute of Technology (KIT), Institute of Organic Chemistry (IOC), Kaiserstrasse 12, Karlsruhe 76131, Germany*
[e] *Indian Institute of Technology Guwahati (IITG), Department of Chemistry, Assam, 781039, India*
[f] *Karlsruhe Institute of Technology (KIT), Institute of Nanotechnology (INT), Hermann-von-Helmholtz Platz-1, Eggenstein-Leopoldshafen 76344, Germany*
[g] *Indian Institute of Technology Guwahati (IITG), Centre for Nanotechnology, Assam, 781039, India*

† Electronic supplementary information (ESI) available: Detailed synthetic protocol and characterization information, along with simulation results. See DOI: https://doi.org/10.1039/d4mh00899e

‡ E. B. and M. L. contributed equally.

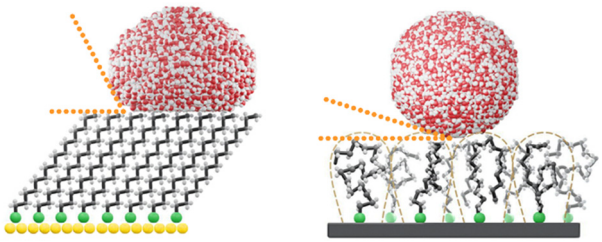

Scheme 1 The water contact angle (WCA) on a hydrocarbon monolayer is shown to be substantially increased when instead of the normal close packing (left) the chains adopt a brush-like structure (right). The C18 hydrocarbon chains have an end-to-end distance of ~2 nm,[17,18] which is much larger than the separation of grafting sites in the SURMOF grid (~0.8 nm), such that the grafted hydrocarbons form a polymer brush.

expose anchoring sites with distances substantially larger than those for other types of substrates.

One of the most important properties of surfaces is their wettability by solvents, most importantly water. The hydrophobic effect during the self-assembly of macromolecules has been recognized as one of the major driving forces in structural pattern formation as protein folding and the "enthalpy–entropy compensation" mechanism in biomaterials.[13,14] Inversely, we demonstrate here that grafting alkyl chains to MOF outer surfaces yields an unusual form of self-assembled monolayers, where the hydrocarbon chains adopt a brush-like structure, to engineer entropic driven superhydrophobic performance. Similar to the case of polymer brushes, entropy contributions from the coiled chains cause a large contact angle for "poor solvents".[15] In contrast to a "good solvent" scenario where a polymer brush is stretched upon mixing, for a poor solvent, the entropic effects feature the formation of collapsed polymer brushes.[16] The key requirement for such brush-like self-assembled monolayers (SAMs) to be formed is an increased spacing of the hydrocarbon chains, as schematically depicted in Scheme 1. While SAMs formed on conventional substrates with rather close spacing of anchoring sites yield low-entropy hydrophilic states, large spacings are required to support the new brush-like state.

We demonstrate the formation of such brush-like SAMs using a particular, highly water-stable MOF family referred to as UiO-66. Recently, several groups have reported strategies to fabricate high-quality thin films of this MOF class,[19] thus allowing the utilization of the external surfaces of this highly interesting type of MOF. Recent studies include the fabrication of hydrophobic MOF particles as detailed by Roland Fischer and coworkers[20] and the exploration of hydrophobization of 2D MOF nanosheets through surface-initiated polymerization.[21] Superhydrophobic, monolithic MOF thin films with low roughness have not yet been reported. In this work, we focus on a particularly attractive member of the UiO-66 family, referred to as UiO-66-NH_2 (Fig. 1). The amino functionality exposed by the linkers of this particular MOF allows attaching further functionalities after MOF formation using straightforward coupling reactions. Eventually, this chemical approach allowed us to attain superhydrophobicity on a crystalline and porous substrate. When we increase the

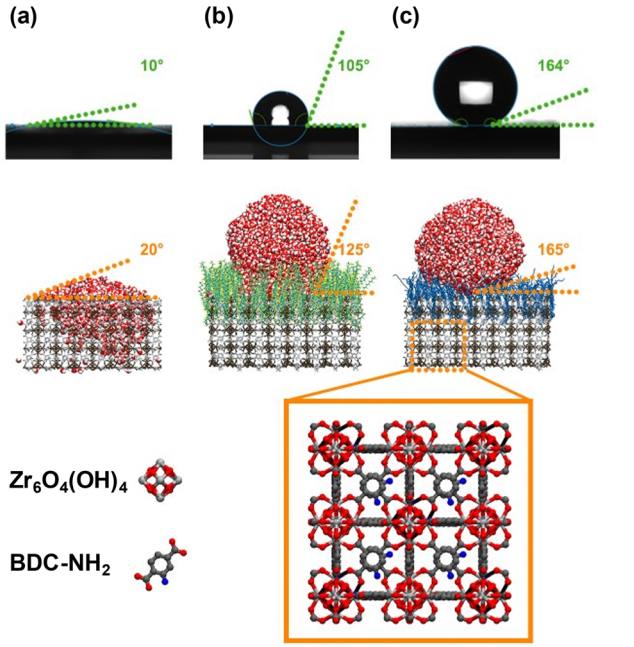

Fig. 1 Static water contact angle; snapshots taken from equilibrated MD-simulations for water droplets and the enlarged structure of UiO-66-NH_2. Top: Static water contact angle of the (a) pristine UiO-66-NH_2 SURMOF, (b) SURMOF grafted with perfluorinated chains, UiO-66-NH-CF and (c) SURMOF grafted with C18 hydrocarbon chains from the experiment and the simulation. Center: Snapshots taken from equilibrated MD-simulations for water droplets on the (a) pristine UiO-66-NH_2 SURMOF, (b) SURMOF grafted with perfluorinated C18F hydrocarbon chains, and (c) SURMOF grafted with C18 hydrocarbon chains. Bottom: Enlarged structure of the UiO-66-NH_2 ($C_{48}H_{34}N_6O_{32}Zr_6$) SURMOF, formed by linking Zr-clusters ($Zr_6O_4(OH)_4$) with organic linkers BDC-NH_2 ($C_8H_7NO_4$). Explicit hydrogen atoms are omitted for clarity.

roughness from the lowest values possible for such UiO-66-NH_2 SURMOFs, 31.4 nm, to larger values, we observe a pronounced reduction in the water adhesion force as measured using a dedicated experimental setup. Such low-adhesion superhydrophobic surfaces carry enormous potential with regard to achieving superior self-cleaning performance. In combination with the low (below 100 nm) roughness such interfaces will prevent the accumulation of submicron-sized solid particulates—unlike conventional high-roughness superhydrophobic interfaces.[22] In fact, there are few reports of superhydrophobic surfaces with low roughness in the literature, as shown in Table S1 (ESI†). A notable example is MOF thin films with a roughness of 80 nm, which exhibit slippery properties even though the water contact angle is only 112 degrees.[23]

Results and discussion

X-ray diffraction (XRD) data recorded for UiO-66-NH_2, UiO-66-NH-C18, and UiO-66-NH-C18F samples revealed that these SURMOFs (surface-mounted metal–organic frameworks) were of high quality and exhibited a high degree of orientation. As shown in the ESI† (Fig. S3a), the XRD peak positions and intensities were fully consistent with the simulations assuming

the previously reported UiO-66-NH_2 bulk structure.[24] After the amidation reaction, the XRD patterns displayed no evident loss in crystallinity, implying that the post-synthetic modification had no impact on the integrity of UiO-66-NH-C_{18} (C18@SURMOF). FT-IR spectroscopy was subsequently employed to confirm the successful grafting of alkyl chains to the SURMOF surface. IRRAS data recorded for the C18@SURMOF shown in Fig. S3b (ESI†) clearly reveals symmetric (2920 cm^{-1}) and asymmetric (2850 cm^{-1}) stretching vibrations of alkyl $-CH_2-$ groups, which were absent in the IR spectra of pristine UiO-66-NH_2. Importantly, the asymmetric and symmetric peaks are shifted by 5 cm^{-1} with respect to "normal" C18 SAMs formed on Au substrates (see Fig. S4 in the ESI†), revealing the presence of a substantial amount of gauche-conformations in the SAM-forming monomers.[25–27] Furthermore, characterization of the three sample types—UiO-66NH_2, C18@UiO-66NH_2, and C18F@UiO-66NH_2—was performed using variable-photon-energy X-ray photoelectron spectroscopy (XPS) (see Fig. S12, ESI†). Despite significant charging issues, we determined a ratio of grafted C18 to C18F chains at 1.4. The lower density of fluorinated chains results from their reduced flexibility, which diminishes the efficiency of the amidation reaction.

As evident from Fig. 1a, for the pristine SURMOF, the static water contact angle is rather small, less than 11°. This strong wetting is expected, as the partially hydroxylated zirconia clusters exposed at the UiO-66 outer surfaces should result in a wetting behavior similar to that of metal oxides.[28] Drastic changes in the wetting properties are observed after grafting C18 alkyl chains to the crystalline array of anchoring sites provided at the outer surface of the porous SURMOF substrate. As shown in Fig. 1c, the surface becomes superhydrophobic, with a static water contact angle (WCA) of larger than 160°.

The analysis of the current C18@SURMOF system using atomic force microscopy (AFM, see Fig. 2a) demonstrates that after the grafting of the hydrocarbon chains the roughness (arithmetic average, R_a) amounts to ~30 nm (see Fig. 2a and Fig. S5, ESI†). Interestingly, the WCA value amounts to ~154°, thus demonstrating the superhydrophobic character of these substrates. To fully characterize surface wetting, it is essential to measure the contact angle hysteresis, the difference between

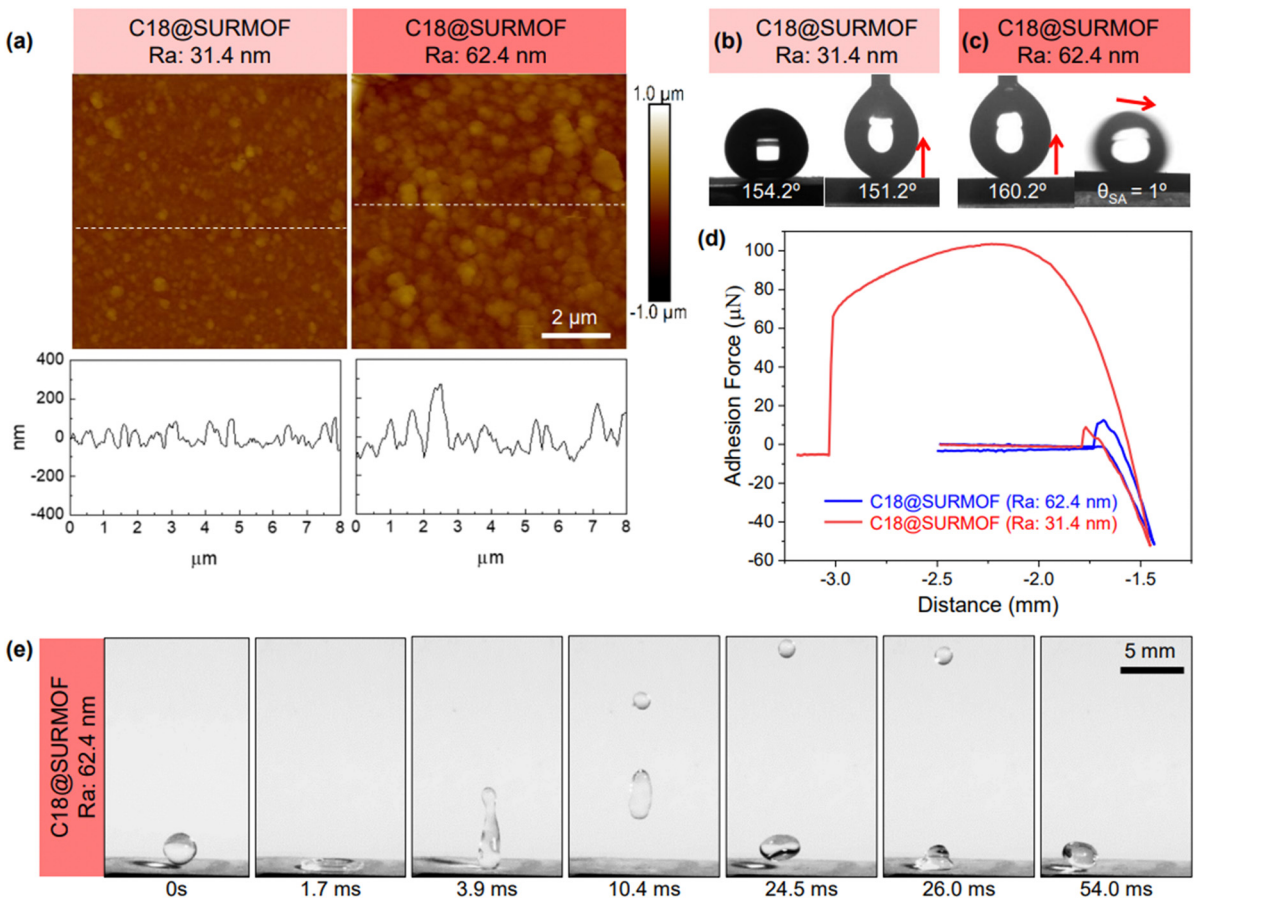

Fig. 2 (a) AFM images comparing the surface roughness of two different C18@SURMOF surfaces. (b) Sequential images showing the static and receding water contact angles on the C18@SURMOF with an average roughness (R_a) of 31.4 nm. The upward arrow indicates the receding of the beaded water droplet. (c) Sequential images showing the receding contact angle and sliding angle on the C18@SURMOF with a R_a of 62.4 nm. The slanting arrow indicates the rolling of the beaded water droplet. (d) Adhesion force measurement of the beaded water droplet on superhydrophobic C18@SURMOF surfaces with R_a values of 31.4 nm (adhesive) and 62.4 nm (non-adhesive). (e) High-speed digital images depict the bouncing behavior of a water droplet dropped on the non-adhesive superhydrophobic C18@SURMOF surface with a R_a of 62.4 nm.

advancing and receding contact angles. For our C18@SURMOF substrates, we found significant hysteresis, with advancing angles around 163° and receding at 151°. However, increasing the R_a from 31.4 nm to 62.4 nm reduced the hysteresis to below 5°, suggesting a notable decrease in water adhesion strength with increasing roughness (see Fig. 2b and c).[29,30]

An independent confirmation of how roughness reduces the adhesion strength of water droplets (volume = 5 μL; Fig. 2d) was provided using a force-tensiometer system equipped with a micro-electromechanical balance.[31] The adhesion decreased significantly from 106.3 ± 5.4 μN to 16.4 ± 4.2 μN as the roughness increased to 62 nm. Additionally, the substrate exhibited an extremely low sliding angle (θ_{SA} = 1°, see Fig. 2c), ensuring the effortless and no-loss rolling of water droplets. Moreover, the dynamics of water droplets impinging on the SURMOF showed almost complete bouncing back (Fig. 2e). These results demonstrate the presence of a superhydrophobic, non-sticky surface. Notably, such non-adhesive superhydrophobicity typically indicates the presence of high-roughness (>100 nm, Table S1, ESI†) substrates with micro- or nanostructures, where air pockets form between the rough surface and liquid, creating the Cassie–Baxter state.[32–35]

The WCA values are much larger than those observed on other hydrocarbon-terminated surfaces, *e.g.*, polyethylene (96°),[36] self-assembled monolayers on Au-substrates (Au-SAMs) made from alkanethiols (109°–112°),[37] alkylsilanes (80°–120°),[38] and polysiloxanes (107°),[39] popular materials for achieving hydrophilic and hydrophobic surfaces.[40–42] Although the roughness of the present samples (30 nm) is higher than that of other systems (sub-10 nm), the WCA values are larger than those of any other substrate with low roughness (below 100 nm) reported in the literature and thus strongly indicates an unusual mechanism yielding superhydrophobicity.

This conclusion is supported by comparisons with two similar recently evaluated substrates. Firstly, an alkylsilane-modified MOF thin film with a roughness of 73.9 nm displayed only moderate hydrophobicity, achieving a WCA of 112°.[23] Secondly, superhydrophobic MOF powder-based films with a much higher roughness of several micrometers showed a WCA value of 156°,[43] which is close to the 154.7° of our low-roughness films but considerably less than the 165° observed in our rough (1 micrometer roughness) C18@SURMOF substrates.

Furthermore, the WCA values of our C18@SURMOF thin films exceeded those of fluoroalkylsilane-coated boehmite transparent thin films, which have roughness (R_a) values around 100 nm and reported WCAs of 150°.[44]

In the present case, fluorination—specifically replacing C18 with C18F—leads to a substantial decrease in the water contact angle instead of the expected increase (see Fig. 1b). This observation, combined with our other findings, consistently suggests an unusual microscopic origin of the superhydrophobicity observed for the C18@SURMOF substrates. Indeed, an obvious difference to conventional SAM/Au systems is the spacing of the hydrocarbon chain anchoring sites. As indicated schematically in Scheme 1, for SAMs on Au(111), these values amount to about 0.4 nm,[25] yielding a tight packing forcing the chains to adopt an all-trans conformation. The SURMOF outer surfaces feature nearly double the chain spacing, allowing more flexibility for individual hydrocarbon chains. This led us to believe that the unexpected superhydrophobicity reported here is due to entropic effects, not static energy, a theory validated by molecular dynamics (MD) simulations.

To verify the hypothesis that entropic effects are responsible for the superhydrophobicity reported here, we carried out a comprehensive series of MD simulations, adhering to schemes that have been previously established.[45–47] For the SURMOF-based system, the simulations were performed by anchoring C18 hydrocarbons to the points of a grid defined by the NH_2 groups exposed at the [001] surface of the SURMOF. The details of the simulations are described in the ESI.† The wetting simulations were carried out by placing a droplet of water on the different substrates. For the C18@SURMOF substrate, the theoretical results revealed strong hydrophobic interactions, with a WCA value of 165°, in full accord with the experimental findings.

To validate our theoretical approach, a number of additional MD simulations were carried out for reference systems. For alkanethiolate-based SAMs on Au(111), we yielded a contact angle of 108°, fully in line with previously reported experimental and theoretical values.[25] For the pristine, bare SURMOF, a low WCA angle of 16° was observed in the simulations, consistent with the behavior expected for a metal oxide cluster-terminated surface (Fig. 1a). In the latter case, snapshots of the wetting simulations reveal that parts of the water droplet actually penetrate into the UiO-66-NH_2 SURMOF, whereas for the C18@SURMOF, the droplet is repelled from the surface to maintain its spherical shape (Fig. 3).

After demonstrating that the simulations fully reproduce the experimental findings, we focused on unraveling the microscopic origins of this unusual hydrophobicity. A detailed analysis confirmed the earlier findings in the SAM@Au case, in that the lowest energy state is one in which alkyl chains are rigidly packed into an array of tilted, by 30°, all-trans chains with a low density of *gauche* conformations. Interestingly, in such SAMs on Au, at elevated temperatures above 80 °C, an order–disorder transition occurs in the outermost segments.[48] This pre-melting can be described by introducing *gauche* defects at the end of chains.

In pronounced contrast, for the case of the C18@SURMOF, the simulations reveal that the hydrocarbon chains adopt a

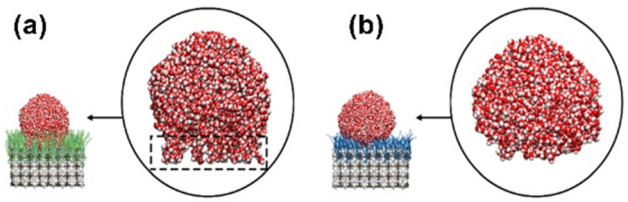

Fig. 3 Snapshots of conformations of the water droplets on the grafted SURMOF with (a) perfluorinated hydrocarbons and (b) C18 hydrocarbons. The dashed region corresponding to the wetting on perfluorinated hydrocarbons exhibits pin-and-plug patterns, mixing with CF chains, whereas in the case of CH chains, the water droplet maintains its spherical shape.

coiled structure, with the density of *gauche* defects increased to 2.89 per hydrocarbon chain. This value is almost as high as that in the high entropy state of free C18 hydrocarbon tangles solvated in a poor solvent like ethanol.[48] As a result of the repulsive interaction with the water droplet, these grafted C18 ''brushes'' are distorted to yield dimples (see Movie S1 in the ESI†). This structural deformation upon contact with water is accompanied by hydrocarbon chains adopting a more stretched configuration with a corresponding entropy penalty, where coil-like hydrocarbon chains trade-off their flexibility to accommodate the water droplet. Such dimples were not observed in the SAM@Au films supporting a water droplet, as expected from the fact that hydrocarbon chains are already fully stretched and tightly packed prior to water droplet deposition.

We, therefore, concluded that entropy contributions must cause the pronounced difference in wetting between the spaced-out (SURMOF substrates) and rigidly packed (SAMs on Au) hydrocarbon chain arrays. This aligns with the finding that fluorination reduces the large WCA angles. In the C18F@SURMOF, the energy cost of forming *gauche* defects in perfluorinated chains is high, inhibiting coiling essential for the C18@SURMOF's superhydrophobicity.

Entropic penalties accompanying the stretching of hydrocarbon chains have been discussed earlier for polymer brushes in non-aqueous environments.[49–51] In particular, Dimitrov *et al.* reported dimple formation when chains in a high entropy state were brought into contact with a bad solvent.[52] The characteristic protrusion observed here for water (a bad solvent) is in full accord with this previous work. The crucial role of entropy in the wetting of related systems, large polymer brushes, was addressed in a recent paper, by Mensink *et al.*[15] Although in these previous simulations the number of segments ($\sim$1000) was almost two orders of magnitude larger than here (18), the analysis of our simulations reveals that the key conclusions from Mensink *et al.* also apply to our system. As indicated in Fig. S7 and S8 (ESI†), despite being a bad solvent, water partially penetrates the arrayed hydrocarbons, thus reducing the conformational space available to the polymer chain.

To allow for quantitative comparison, we have computed the conformational entropy for SAM@Au, the C18@SURMOF, and C18F@SURMOF (with perfluorinated chains) as defined by $S = -\sum_i p_i \ln p_i$ where p_i corresponds to the occurrence frequencies of conformers in Ramachandran plots (Fig. S9, ESI†). We found that S = 5.3k_b, 6.47k_b, and 6.97k_b for the SAM, C18F@SURMOF, and C18@SURMOF, respectively. The largest conformational entropy is thus observed for C18F@SURMOF films, consistent with the fact that the interaction with the ''bad solvent'' H_2O leads to the largest water contact angles. In the C18F@SURMOF case, forming *gauche* defects in CF chains is accompanied by a substantially stronger energy penalty than for CH chains, thus aligning most CF groups into a *trans* conformation. As a result, the influence of entropy is substantially smaller, as illustrated in Fig. 3 and Fig. S9 (ESI†). The lower density of *gauche* defects is also reflected by an increased adlayer thickness (+0.4 nm) for the perfluorinated case (Fig. 1 and Fig. S7, ESI†). Additionally, in contrast to the Cassie–Baxter wetting state, water molecules are able to penetrate between CF chains to reach the underlying SURMOF, to enable wetting in the Wenzel state.[53] Here, the water forms pin-like structures that plug into CF bushes (Fig. 3), consistent with previous reports on a planar substrate.[45] As a result, the less flexible CF chains, with a less intrinsic entropy, mix better with water. This Wenzel-state wetting results in the contact angle reduction of the fluorinated SAM on the SURMOF surface to around 120°.

To summarize, MD simulations reveal the hydrophilic and hydrophobic characteristics of the pristine SURMOF, C18F@SURMOF, and C18@SURMOF, respectively. The non-adhesive superhydrophobic behavior of the C18@SURMOF results from the high intrinsic entropy in the C18 hydrocarbon chains grafted at the distances defined by the MOF lattice. Long-term experiments revealed an impressive stability of this non-adhesive superhydrophobicity on a low-roughness interface; even after 90 days no substantial changes in the contact angle could be observed.

Conclusion

This study reports the successful fabrication of superhydrophobic surfaces by grafting C18 hydrocarbon chains to UiO-66-NH_2 monolithic MOF thin films. Originally, the SURMOFs showed strong wetting, with water contact angles (WCAs) below 11°. However, these surfaces became superhydrophobic after post-functionalization, with WCAs as high as 165°. Notably, replacing the C18 chains with their fluorinated counterparts did not increase but rather decreased the water contact angles, suggesting that the residual 30 nm roughness of the C18@SURMOF monolithic thin films alone does not account for the exceptionally high WCA observed. Molecular dynamics (MD) identified another origin, namely, entropic effects of coiled C18 chains. In excellent agreement with the experiments, the simulations yielded a WCA value of 165° for the C18@SURMOF even in the absence of surface roughness, whereas the perfluorinated cases exhibited a significantly lower water contact angle of 123°.[54] The entropy-related superhydrophobicity of alkyl-chains grafted to a grid with large spacing described here should also apply to other MOF surfaces and will be the topic of further research.

Additionally, it was found that manipulating the roughness of the SURMOFs could modulate the water adhesion strength. Low roughness levels ($\sim$30 nm) resulted in higher adhesion strengths, evidenced by notable differences between the advancing and receding contact angles and in the water adhesion forces (16.4 $\pm$ 4.2 μN *vs.* 106.3 $\pm$ 5.4 μN). Conversely, increasing the roughness in the nanometric range significantly reduced the contact angle hysteresis and decreased the adhesion strength by roughly an order of magnitude.

Moreover, while the prepared superhydrophobic thin film repelled beaded water extremely, the droplet of oil readily spread with contact angles $<$10°. In the past, such selective wettability has been strategically utilized for oil–water separation.[55–57]

Given the plethora of surface structuring techniques available for SURMOFs, such as photo- and e-beam lithography, these newly functionalized surfaces are poised to greatly impact the creation of hydrophilic/hydrophobic nano- or micro-structured surfaces.[58] Furthermore, the emergence of superhydrophobic substrates with low adhesion strength heralds various potential applications, notably with regard to the fabrication of self-cleaning surfaces.[22,59]

Author contributions

All authors have given approval to the final version of the manuscript.

Data availability

All data relevant to our paper are either provided in the ESI† or are available from the authors on request.

Conflicts of interest

The authors declare no conflicts of interest.

Acknowledgements

T. H., M. L., P. L., S. B., W. W., and C. W. acknowledge support from the Deutsche Forschungsgemeinschaft (DFG, German Research Foundation) under the Germany Excellence Strategy *via* the Excellence Cluster 3D Matter Made to Order (grant no. EXC-2082/1-390761711); M. L., W. W., and C. W. acknowledge support *via* the Helmholtz Joint Lab "Virtual Materials Design" (VMD). P. A. L. thanks the Deutsche Forschungsgemeinschaft (DFG) (Heisenbergprofessur project number 406232485, LE 2936/9-1. U. M. acknowledges the International Excellent Fellowship of KIT, Germany. The authors acknowledge the support of Dr Alexei Nefedov in XPS measurements and data analysis. Additionally, M. L. expresses special thanks to Dr Saietan Bag for the helpful suggestions in building the molecular dynamics model. The Helmholtz Zentrum Berlin für Materialien und Energie (HZB) is gratefully acknowledged for beamtime allocation and technical assistance.

References

1 S. Kitagawa, R. Kitaura and S.-I. Noro, Functional Porous Coordination Polymers, *Angew. Chem., Int. Ed.*, 2004, **43**(18), 2334–2375, DOI: 10.1002/anie.200300610.

2 A. Ahmed, S. Seth, J. Purewal, A. G. Wong-Foy, M. Veenstra, A. J. Matzger and D. J. Siegel, Exceptional Hydrogen Storage Achieved by Screening Nearly Half a Million Metal–Organic Frameworks, *Nat. Commun.*, 2019, **10**(1), 1568, DOI: 10.1038/s41467-019-09365-w.

3 M. Ding, R. W. Flaig, H.-L. Jiang and O. M. Yaghi, Carbon Capture and Conversion Using Metal–Organic Frameworks and MOF-based Materials, *Chem. Soc. Rev.*, 2019, **48**(10), 2783–2828, DOI: 10.1039/C8CS00829A.

4 Q. Qian, P. A. Asinger, M. J. Lee, G. Han, K. Mizrahi Rodriguez, S. Lin, F. M. Benedetti, A. X. Wu, W. S. Chi and Z. P. Smith, MOF-Based Membranes for Gas Separations, *Chem. Rev.*, 2020, **120**(16), 8161–8266, DOI: 10.1021/acs.chemrev.0c00119.

5 D. Yang and B. C. Gates, Catalysis by Metal Organic Frameworks: Perspective and Suggestions for Future Research, *ACS Catal.*, 2019, **9**(3), 1779–1798, DOI: 10.1021/acscatal.8b04515.

6 V. Pascanu, G. González Miera, A. K. Inge and B. N. Martín-Matute, Metal–Organic Frameworks as Catalysts for Organic Synthesis: a critical perspective, *J. Am. Chem. Soc.*, 2019, **141**(18), 7223–7234.

7 L. S. Xie, G. Skorupskii and M. Dincă, Electrically Conductive Metal–Organic Frameworks, *Chem. Rev.*, 2020, **120**(16), 8536–8580, DOI: 10.1021/acs.chemrev.9b00766.

8 M. D. Allendorf, R. Dong, X. Feng, S. Kaskel, D. Matoga and V. Stavila, Electronic Devices Using Open Framework Materials, *Chem. Rev.*, 2020, **120**(16), 8581–8640, DOI: 10.1021/acs.chemrev.0c00033.

9 R. Haldar, M. Jakoby, M. Kozlowska, M. Rahman Khan, H. Chen, Y. Pramudya, B. S. Richards, L. Heinke, W. Wenzel and F. Odobel, *et al.*, Tuning Optical Properties by Controlled Aggregation: Electroluminescence Assisted by Thermally-Activated Delayed Fluorescence from Thin Films of Crystalline Chromophores, *Chem. – Eur. J.*, 2020, **26**(71), 17016–17020, DOI: 10.1002/chem.202003712.

10 M. Brattoli, G. De Gennaro, V. De Pinto, A. D. Loiotile, S. Lovascio and M. Penza, Odour detection methods: Olfactometry and chemical sensors, *Sensors*, 2011, **11**, 5290–5322.

11 S. Bundschuh, O. Kraft, H. Arslan, H. Gliemann, P. Weidler and C. Wöll, Mechanical properties of metal–organic frameworks: An indentation study on epitaxial thin films, *Appl. Phys. Lett.*, 2012, **101**(10), 101910.

12 D. H. Chen, A. E. Sedykh, G. E. Gomez, B. L. Neumeier, J. C. C. Santos, V. Gvilava, R. Maile, C. Feldmann, C. WÖll and C. Janiak, *et al.*, SURMOF Devices Based on Heteroepitaxial Architectures with White-Light Emission and Luminescent Thermal-Dependent Performance, *Adv. Mater. Interfaces*, 2020, **7**(24), 2000929, DOI: 10.1002/admi.202000929.

13 Q. Sun, The Hydrophobic Effects: Our Current Understanding, *Molecules*, 2022, **27**, DOI: 10.3390/molecules27207009.

14 M. Schauperl, M. Podewitz, B. Waldner and K. Liedl, Enthalpic and Entropic Contributions to Hydrophobicity, *J. Chem. Theory Comput.*, 2016, **12**, 4600–4610, DOI: 10.1021/acs.jctc.6b00422.

15 L. I. Mensink, S. de Beer and J. H. Snoeijer, The role of entropy in wetting of polymer brushes, *Soft Matter*, 2021, **17**(5), 1368–1375.

16 L. Mensink, J. Snoeijer and S. de Beer, Wetting of Polymer Brushes by Polymeric Nanodroplets, *Macromolecules*, 2019, **52**, 2015–2020, DOI: 10.1021/acs.macromol.8b02409.

17 C. Y. Zhao, Y. B. Tao and W. Y. Wang, Shell effect on microstructure and diffusion in interface region of nanoencapsulated phase change material: A molecular dynamics simulation, *J. Mol. Liq.*, 2022, **354**, 118872, DOI: 10.1016/j.molliq.2022.118872.

18 M. Abbaspour, M. N. Jorabchi, H. Akbarzadeh and A. Ebrahimnejad, Investigation of the thermal properties of phase change materials encapsulated in capped carbon nanotubes using molecular dynamics simulations, *RSC Adv.*, 2021, **11**(40), 24594–24606, DOI: 10.1039/D1RA02033A.

19 A. L. Semrau and R. A. Fischer, High-Quality Thin Films of UiO-66-NH2 by Coordination Modulated Layer-by-Layer Liquid Phase Epitaxy, *Chemistry*, 2021, **27**(33), 8509.

20 K. Joyaramulu, F. Geyer, A. Schneemann, S. Kment, M. Otyepka, R. Zboril, D. Vollmer and R. Fischer, Hydrophobic Metal–Organic Frameworks, *Adv. Mater.*, 2019, **31**, 1900820, DOI: 10.1002/adma.201900820.

21 S. Ye, N. Hosono and T. Uemura, Polymer-Grafting from MOF Nanosheets for the Fabrication of Versatile 2D Materials, *Adv. Funct. Mater.*, 2024, **34**, 2312265, DOI: 10.1002/adfm.202312265.

22 F. Geyer, M. D'Acunzi, A. Sharifi-Aghili, A. Saal, N. Gao, A. Kaltbeitzel, T. F. Sloot, R. Berger, H. J. Butt and D. Vollmer, When and how self-cleaning of superhydrophobic surfaces works, *Sci. Adv.*, 2020, **6**(3), eaaw9727, DOI: 10.1126/sciadv.aaw9727.

23 V. Singh, X. H. Men and M. K. Tiwari, Transparent and Robust Amphiphobic Surfaces Exploiting Nanohierarchical Surface-grown Metal–Organic Frameworks, *Nano Lett.*, 2021, **21**(8), 3480–3486, DOI: 10.1021/acs.nanolett.1c00157.

24 D. T. Lee, J. Zhao, C. J. Oldham, G. W. Peterson and G. N. Parsons, UiO-66-NH_2 Metal–Organic Framework (MOF) Nucleation on TiO_2, ZnO, and Al_2O_3 Atomic Layer Deposition-Treated Polymer Fibers: Role of Metal Oxide on MOF Growth and Catalytic Hydrolysis of Chemical Warfare Agent Simulants, *ACS Appl. Mater. Interfaces*, 2017, **9**(51), 44847–44855, DOI: 10.1021/acsami.7b15397.

25 M. Kind and C. Wöll, Organic surfaces exposed by self-assembled organothiol monolayers: Preparation, characterization, and application, *Prog. Surf. Sci.*, 2009, **84**(7–8), 230–278.

26 E. Pensa, C. Vericat, D. Grumelli, R. C. Salvarezza, S. H. Park, G. S. Longo, I. Szleifer and L. P. M. De Leo, New insight into the electrochemical desorption of alkanethiol SAMs on gold, *Phys. Chem. Chem. Phys.*, 2012, **14**(35), 12355–12367.

27 L. Tian, A. Fan, X. Yu and W. Hu, Achieving high-performance molecular rectification through fast screening alkanethiol carboxylate-metal complexes electroactive units, *CCS Chem.*, 2023, **5**(4), 902–914.

28 R. Lundy, C. Byrne, J. Bogan, K. Nolan, M. N. Collins, E. Dalton and R. Enright, Exploring the Role of Adsorption and Surface State on the Hydrophobicity of Rare Earth Oxides, *ACS Appl. Mater. Interfaces*, 2017, **9**(15), 13751–13760, DOI: 10.1021/acsami.7b01515.

29 T. Mouterde, P. S. Raux, C. Clanet and D. Quéré, Superhydrophobic frictions, *Proc. Natl. Acad. Sci. U. S. A.*, 2019, **116**(17), 8220–8223, DOI: 10.1073/pnas.1819979116.

30 M. Reyssat, D. Richard, C. Clanet and D. Quéré, Dynamical superhydrophobicity, *Faraday Discuss.*, 2010, **146**, 19–33, DOI: 10.1039/c000410n.

31 M. Dhar, U. I. Kara, S. Das, Y. Xu, S. Mandal, R. L. Dupont, E. C. Boerner, B. Chen, Y. Yao and X. Wang, *et al.*, Design of a self-cleanable multilevel anticounterfeiting interface through covalent chemical modulation, *Mater. Horiz.*, 2023, **10**(6), 2204–2214, DOI: 10.1039/D3MH00180F.

32 L. Feng, S. H. Li, Y. S. Li, H. J. Li, L. J. Zhang, J. Zhai, Y. L. Song, B. Q. Liu, L. Jiang and D. B. Zhu, Superhydrophobic surfaces: From natural to artificial, *Adv. Mater.*, 2002, **14**(24), 1857–1860, DOI: 10.1002/adma.200290020.

33 E. Bittoun and A. Marmur, The Role of Multiscale Roughness in the Lotus Effect: Is It Essential for Super-Hydrophobicity, *Langmuir*, 2012, **28**(39), 13933–13942, DOI: 10.1021/la3029512.

34 M. Miwa, A. Nakajima, A. Fujishima, K. Hashimoto and T. Watanabe, Effects of the surface roughness on sliding angles of water droplets on superhydrophobic surfaces, *Langmuir*, 2000, **16**(13), 5754–5760, DOI: 10.1021/la991660o.

35 B. Bhushan, Y. C. Jung and K. Koch, Self-Cleaning Efficiency of Artificial Superhydrophobic Surfaces, *Langmuir*, 2009, **25**(5), 3240–3248, DOI: 10.1021/la803860d.

36 J. Victor, D. Facchini, G. Palumbo and U. Erb, Biology inspired superhydrophobic surfaces, *Adv. Mater. Res.*, 2012, 814–819.

37 A. Ulman and N. Tillman, Self-Assembling Double-Layers on Gold Surfaces - The Merging of 2 Chemistries, *Langmuir*, 1989, **5**(6), 1418–1420, DOI: 10.1021/la00090a028.

38 D. A. Stenger, C. J. Pike, J. J. Hickman and C. W. Cotman, Surface Determinants of Neuronal Survival and Growth on Self-Assembled Monolayers in Culture, *Brain Res.*, 1993, **630**(1–2), 136–147, DOI: 10.1016/0006-8993(93)90651-3.

39 J. Y. Kim, E. K. Lee, J. Jung, D. W. Lee, Y. Yun, J. W. Chung, J. I. Park and J. J. Kim, Densely cross-linked polysiloxane dielectric for organic thin-film transistors with enhanced electrical stability, *J. Mater. Chem. C*, 2019, **7**(19), 5821–5829, DOI: 10.1039/c8tc06236f.

40 A. Harsch, J. Calderon, R. Timmons and G. Gross, Pulsed plasma deposition of allylamine on polysiloxane: a stable surface for neuronal cell adhesion, *J. Neurosci. Methods*, 2000, **98**(2), 135–144.

41 G. Lin, X. Zhang, S. R. Kumar and J. E. Mark, Modification of Polysiloxane Networks for Biocompatibility, *Mol. Cryst. Liq. Cryst.*, 2010, **521**(1), 56–71, DOI: 10.1080/15421401003719738.

42 Z. Sun, B. Liu, S. Huang, J. Wu and Q. Zhang, Facile fabrication of superhydrophobic coating based on polysiloxane emulsion, *Prog. Org. Coat.*, 2017, **102**, 131–137, DOI: 10.1016/j.porgcoat.2016.07.003.

43 M. L. Gao, S. Y. Zhao, Z. Y. Chen, L. Liu and Z. B. Han, Superhydrophobic/Superoleophilic MOF Composites for Oil-Water Separation, *Inorg. Chem.*, 2019, **58**(4), 2261–2264, DOI: 10.1021/acs.inorgchem.8b03293.

44 A. Nakajima, A. Fujishima, K. Hashimoto and T. Watanabe, Preparation of transparent superhydrophobic boehmite and silica films by sublimation of aluminum acetylacetonate, *Adv. Mater.*, 1999, **11**(16), 1365–1368, DOI: 10.1002/(sici)1521-4095(199911)11:16<1365::Aid-adma1365>3.0.Co;2-f.

45 H. Li, T. Yan, K. A. Fichthorn and S. Yu, Dynamic contact angles and mechanisms of motion of water droplets moving

on nanopillared superhydrophobic surfaces: a molecular dynamics simulation study, *Langmuir*, 2018, **34**(34), 9917–9926.

46 S. Chen, J. Wang, T. Ma and D. Chen, Molecular dynamics simulations of wetting behavior of water droplets on polytetrafluorethylene surfaces, *J. chem. Phys.*, 2014, **140**(11), 114704.

47 P. Bhadra and S. W. I. Siu, Comparison of Biomolecular Force Fields for Alkanethiol Self-Assembled Monolayer Simulations, *J. Phys. Chem. C*, 2017, **121**(47), 26340–26349, DOI: **10.1021/acs.jpcc.7b08092**.

48 A. Schertel, G. Hahner, M. Grunze and C. Wöll, Near edge x-ray absorption fine structure investigation of the orientation and thermally induced order-disorder transition in thin organic films containing long chain hydrocarbons, *J. Vac. Sci. Technol., A*, 1996, **14**(3), 1801–1806, DOI: **10.1116/1.580339**.

49 T. Saitoh, H. Hoshino and T. Yotsuyanagi, Volume constraint effect on solute partitioning to Triton X-100 micelles in water, *J. Chem. Soc., Faraday Trans.*, 1994, **90**(3), 479–486, DOI: **10.1039/FT9949000479**.

50 A. M. Jonas, Z. J. Hu, K. Glinel and W. T. S. Huck, Chain entropy and wetting energy control the shape of nanopatterned polymer brushes, *Macromolecules*, 2008, **41**(19), 6859–6863, DOI: **10.1021/ma801584k**.

51 K. Binder and A. Milchev, Polymer brushes on flat and curved surfaces: How computer simulations can help to test theories and to interpret experiments, *J. Polym. Sci., Part B: Polym. Phys.*, 2012, **50**(22), 1515–1555, DOI: **10.1002/polb.23168**.

52 D. I. Dimitrov, A. Milchev and K. Binder, Polymer brushes in solvents of variable quality: Molecular dynamics simulations using explicit solvent, *J. Chem. Phys.*, 2007, **127**(8), 084905, DOI: **10.1063/1.2768525**.

53 J. Bico, C. Marzolin and D. Quéré, Pearl drops, *Europhys. Lett.*, 1999, **47**(2), 220–226, DOI: **10.1209/epl/i1999-00548-y**.

54 R. Colorado and T. R. Lee, Wettabilities of Self-Assembled Monolayers on Gold Generated from Progressively Fluorinated Alkanethiols, *Langmuir*, 2003, **19**(8), 3288–3296, DOI: **10.1021/la0263763**.

55 S. Ruidas, A. Das, S. Kumar, S. Dalapati, U. Manna and A. Bhaumik, Non-Fluorinated and Robust Superhydrophobic Modification on Covalent Organic Framework for Crude-Oil-in-Water Emulsion Separation, *Angew. Chem., Int. Ed.*, 2022, **61**, e202210507, DOI: **10.1002/anie.202210507**.

56 Z. Shi, H. Zeng, Y. Yuan, N. Shi, L. Wen, H. Rong, D. Zhu, L. Hu, L. Ji and L. Zhao, *et al.*, Constructing Superhydrophobicity by Self-Assembly of SiO2@Polydopamine Core-Shell Nanospheres with Robust Oil-Water Separation Efficiency and Anti-Corrosion Performance, *Adv. Funct. Mater.*, 2023, **33**, 2213042, DOI: **10.1002/adfm.202213042**.

57 Z. Chu, Y. Feng and S. Seeger, Oil/Water Separation with Selective Superantiwetting/Superwetting Surface Materials, *Angew. Chem., Int. Ed.*, 2015, **54**, 2328–2338, DOI: **10.1002/anie.201405785**.

58 E. Ueda and P. A. Levkin, Emerging Applications of Superhydrophilic-Superhydrophobic Micropatterns, *Adv. Mater.*, 2013, **25**(9), 1234–1247, DOI: **10.1002/adma.201204120**.

59 L. S. Zhang, A. G. Zhou, B. R. Sun, K. S. Chen and H. Z. Yu, Functional and versatile superhydrophobic coatings via stoichiometric silanization, *Nat. Commun.*, 2021, **12**(1), 982, DOI: **10.1038/s41467-021-21219-y**.